Supplemental Information

Supplemental Figures and Legends

Figure S1, Related to Figure 1

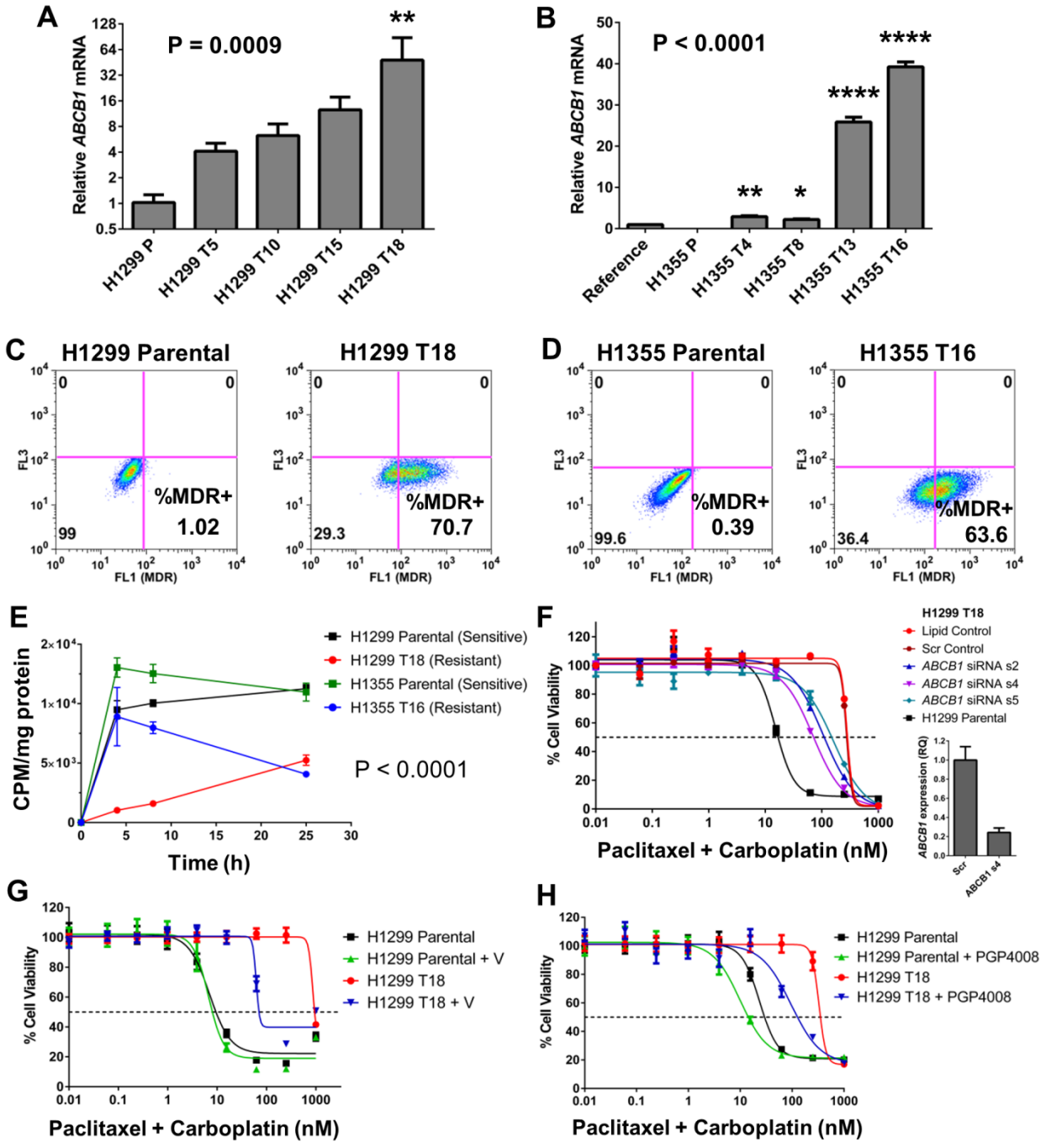

Figure S1. Chemoresistant cells express ABCB1/ MDR1 drug transporter and show partial reversal of resistance upon MDR1 inhibition.

(A, B) H1299 and H1355 resistant cell line series showed increase in *ABCB1* mRNA transcripts with increasing treatment cycles. Data represents mean ± SD. Statistical significance was tested by one-way ANOVA, followed by Dunnett's multiple comparisons test of each resistant variant with the parental cell line (indicated by asterisks). P values on graphs denote significance from post-test for linear trend.

(C, D) H1299 T18 and H1355 T16 showed enrichment in % MDR+ cells (FACS).

(E) H1299 T18 and H1355 T16 resistant cell lines exhibited decreased intracellular accumulation of tritiated docetaxel compared to parental cells. Data represent mean ± SEM. Two-way ANOVA, $P < 0.0001$

(F) siRNA knockdown of ABCB1 (3 individual siRNAs: s2, s4, s5) in H1299 T18 could only partially reverse resistance to paclitaxel + carboplatin. Data represents mean ± SD. Knockdown was validated by decrease in *ABCB1* mRNA (see qPCR data for s4 siRNA).

(G, H) Drug response to paclitaxel + carboplatin was tested in the presence of non-specific MDR inhibitor verapamil (V, 5 μM) or MDR1/Pgp selective inhibitor PGP4008 (10 μM). There was partial shift in drug response curves. Each data-point represents mean ± SD of 8 replicates.

Figure S2, Related to Figure 1

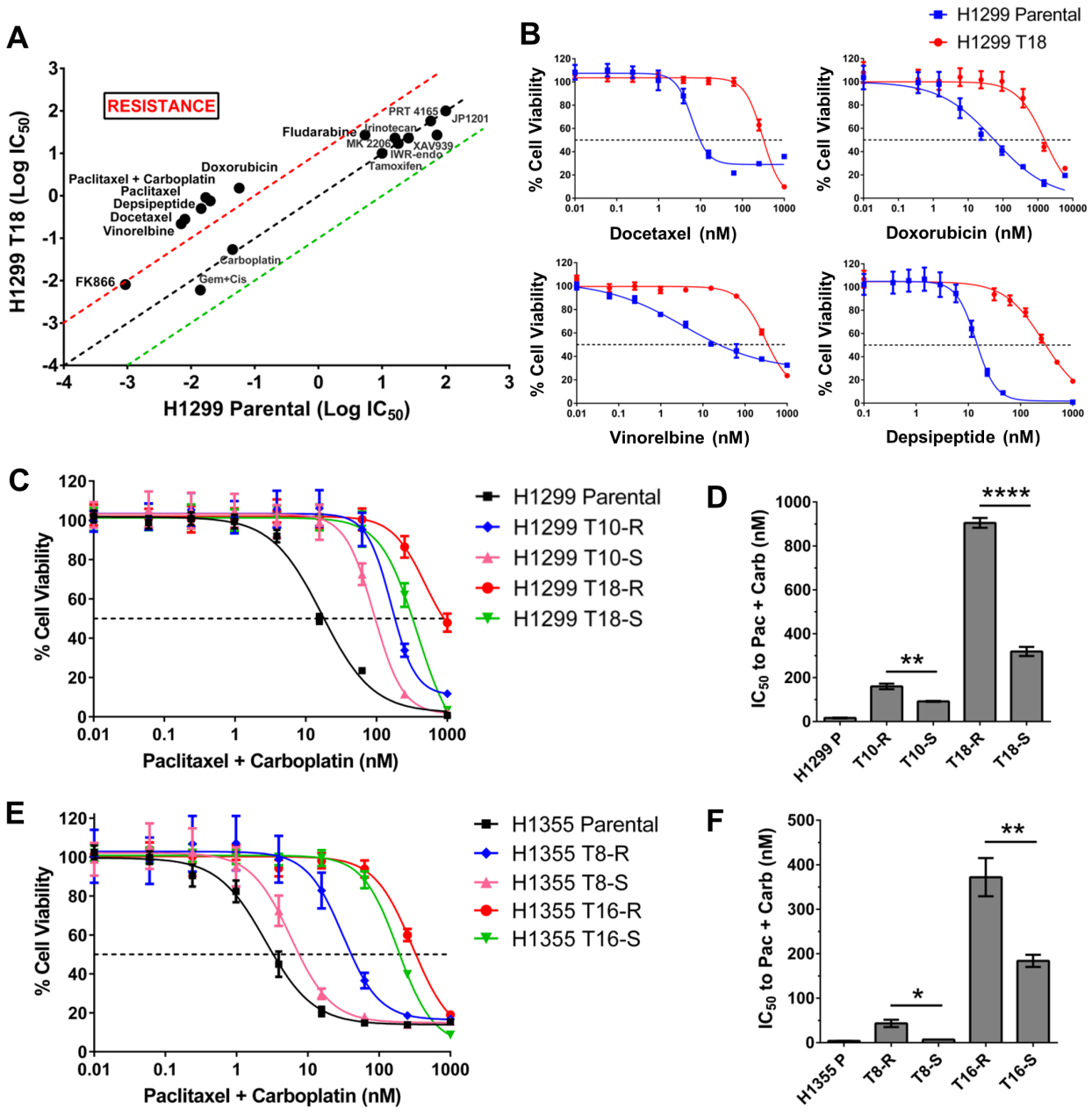

Figure S2. Paclitaxel + carboplatin resistant variants exhibit cross-resistance and display partial reversibility in resistance upon extended drug-free culturing.

(A) H1299 T18 resistant cells showed multi-drug resistance phenotype. Red and green dotted lines indicate 10-fold cut-offs for resistance and sensitivity respectively.

(B) Paclitaxel + carboplatin resistant cell line variants showed cross-resistance to docetaxel, doxorubicin, vinorelbine and depsipeptide. Each data-point represents mean + SD from 8 replicates per drug dose.

(C, E) Dose response curves illustrating partial reversal in chemo-resistance upon drug-free culturing for >4 months. Suffix 'R' denotes resistant cells and 'S' indicates partially re-sensitized cells. Each assay includes 8 replicates per drug dose. Error bars represent mean $\pm$ SD. X-axis shows paclitaxel dose in the 2:3 paclitaxel: carboplatin combination.

(D, F) IC_{50} values from MTS assays ($n \geq 3$) depicting reversal of resistance. Error bars represent mean $\pm$ SEM. P values are from two-tailed unpaired t-test; *P<0.05, **P<0.01, ***P<0.001, ****P<0.0001.

Figure S3, Related to Figure 1

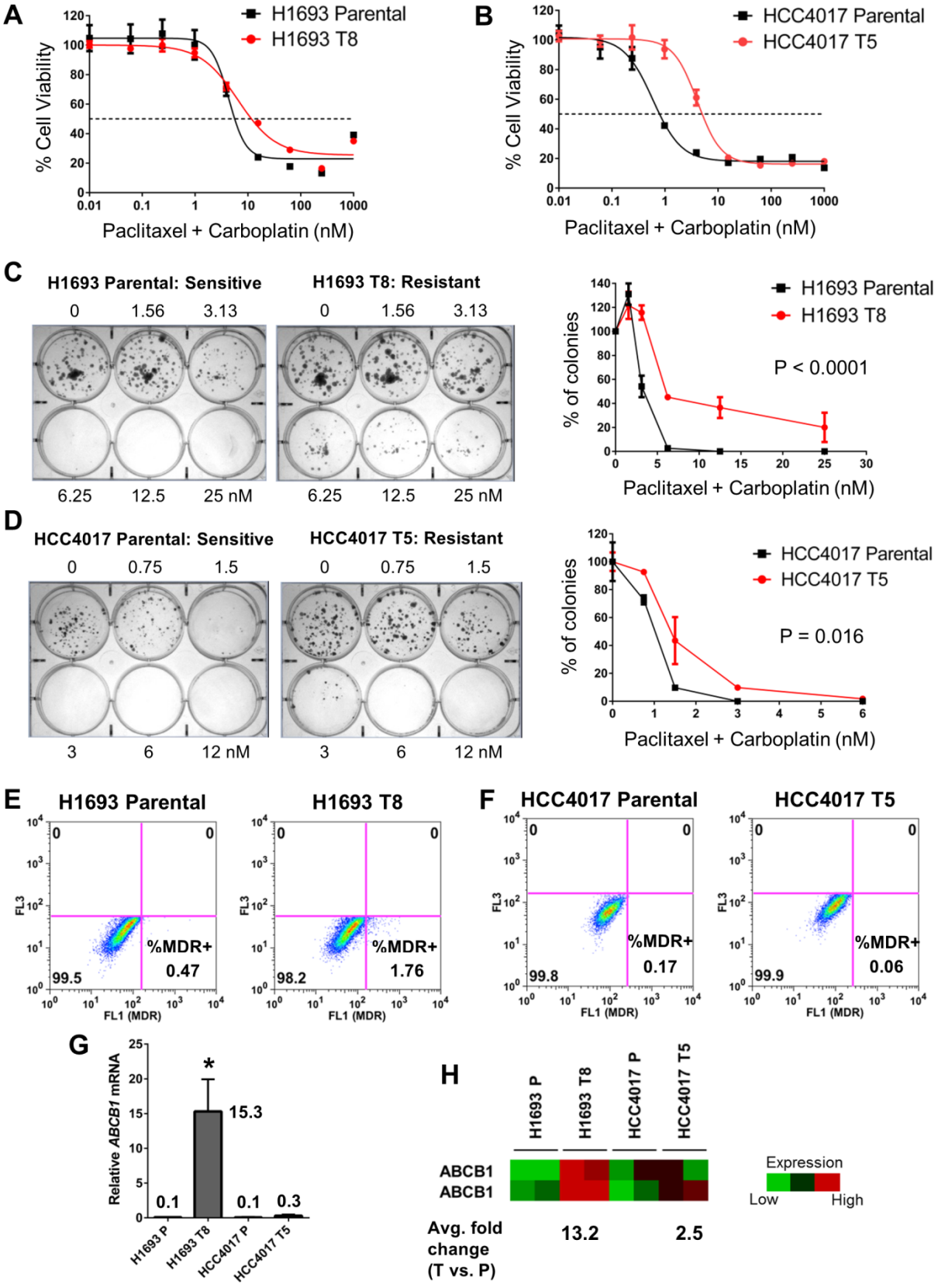

Figure S3. H1693 T8 and HCC4017 T5 cell line variants exhibit paclitaxel + carboplatin resistance, but HCC4017 T5 cells do not show increased MDR1 expression.

(A, B) H1693 T8 and HCC4017 T5 cell line variants were established by long-term treatment of parental cell lines with 8 and 5 cycles respectively of paclitaxel + carboplatin (2:3 wt/wt) doublet. Development of resistance was tested by MTS assays. Values in dose response plots indicate paclitaxel concentration in the doublet. Each assay was performed with 8 replicates per drug dose. Data represents mean $\pm$ SD.

(C, D) Increase in drug resistance was validated by colony formation. Error bars indicate mean $\pm$ SEM. P values are from two-way ANOVA.

(E, F) H1693 T8 showed enrichment in % MDR+ cell subpopulation whereas HCC4017 T5 cells did not show any increase in %MDR1+ cells by flow cytometry.

(G, H) There was significant increase in *ABCB1* mRNA expression in H1693 T8 compared to H1693 Parental, but minimal changes in *ABCB1* transcripts in HCC4017 T5 resistant cells (qRT-PCR and microarray). Error bars in qRT-PCR data represent mean $\pm$ SD. Heat map denotes expression from two *ABCB1* microarray probes and two biological replicates per cell line.

Figure S4, Related to Figure 3

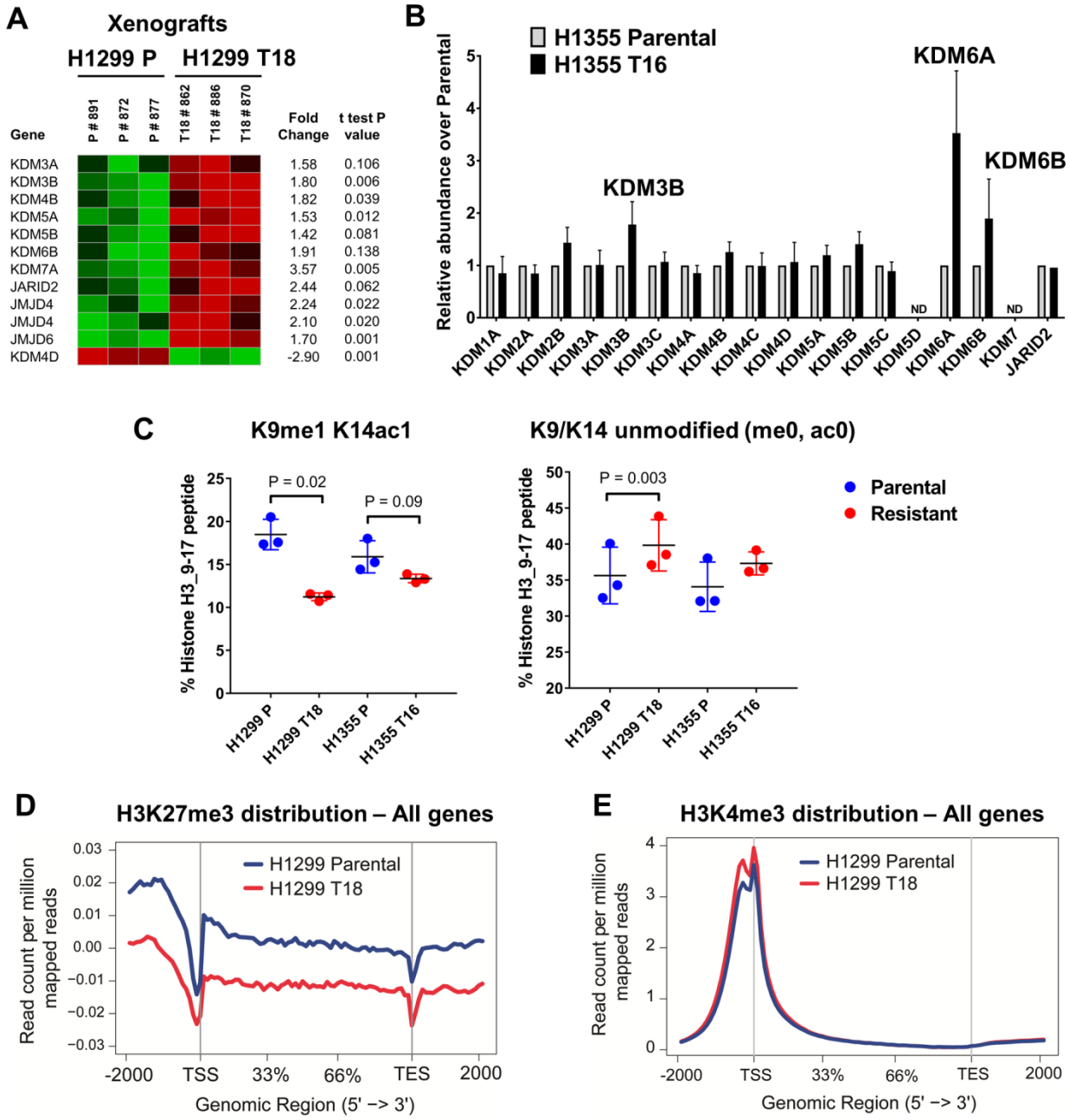

Figure S4. Chemoresistant NSCLC cells exhibit increased KDM expression and altered histone methylation levels by mass spectrometry and ChIP-sequencing.

(A) Heat map representing all differentially expressed KDM transcripts in H1299 T18 vs H1299 Parental xenograft tumors. N = 3 tumors per group, P values are from unpaired t-tests.

(B) H1355 T16 chemoresistant cells show increased expression of mainly KDM3B, KDM6A and KDM6B, compared to H1355 Parental cells by qRT-PCR. Cyclophilin B was used as endogenous control.

(C) Analysis of combinatorial histone PTMs by mass spectrometry revealed that both H1299 T18 and H1355 t16 chemoresistant cells showed decreased H3K9me1 K14ac1 and a corresponding increase in % of H3K9/K14 unmodified (me0/ac0) peptide. Data represents 3 biological replicates per group. P values are from two-tailed unpaired t-tests.

(D) H3K27me3 average distribution across all transcribed regions of the genome by ChIP-seq, showing an overall decrease in H3K27me3 enrichment in H1299 T18 compared to H1299 Parental cells.

(E) H1299 T18 cells did not show any decrease in average H3K4me3 ChIP-seq distribution across transcribed regions of the genome, when compared with H1299 Parental cells.

For both (D) and (E), average H3K27me3 or H3K4me3 ChIP read depth in the gene body regions and 2kb 5' and 3' to the gene body regions was subtracted from respective input read depth and plotted. X-axis represents the genomic regions from 5' to 3' and the Y-axis represents read depth. TSS, transcription start site; TES, transcription end site.

Figure S5, Related to Figure 4

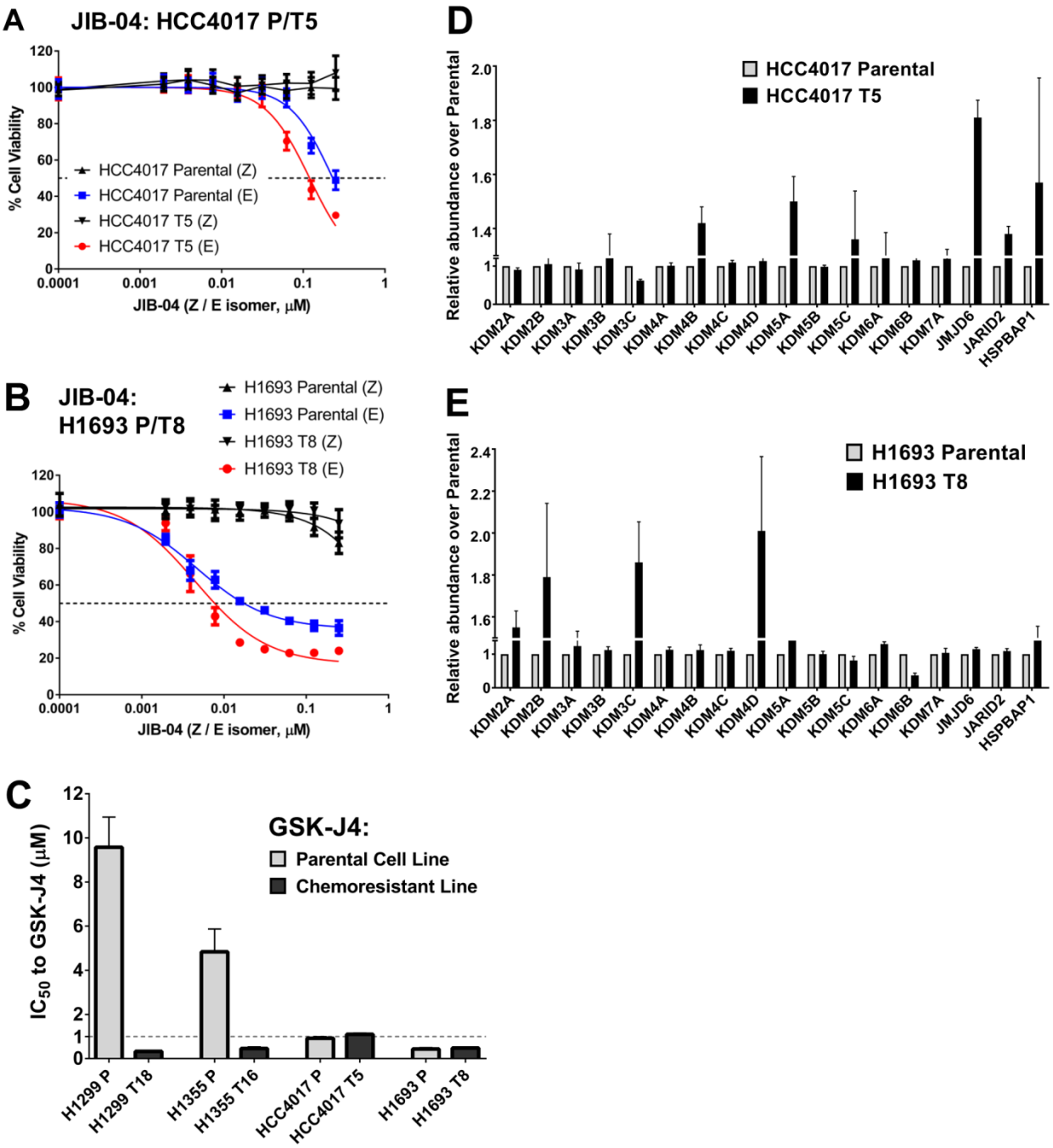

Figure S5. HCC4017 T5 and H1693 T8 chemoresistant cells show increased sensitivity to the pan-KDM inhibitor JIB-04, but not to the KDM6 specific inhibitor GSK-J4.

(A, B) HCC5017 T5 and H1693 T8 cells which were ~3-fold resistant to paclitaxel + carboplatin (see Figure S3) showed ~3-fold increased sensitivity to the pan-JmjC KDM inhibitor JIB-04, compared to corresponding parental cell lines. 'E' indicates JIB-04 active isomer, 'Z' is the inactive isomer. Each data point represents mean $\pm$ SD of 8 replicates.

(C) GSK-J4 IC_{50} values from multiple experiments, showing that hyper-sensitization to this KDM6 inhibitor was only seen in H1299 T18 and H1355 T16 resistant variants, and not in HCC4017 T5 or H1693 T8 resistant variants.

(D) HCC4017 T5 showed up-regulation of other KDMs (not KDM6A/6B), when compared to HCC4017 Parental cells by qRT-PCR.

(E) H1693 T8 showed up-regulation of other KDMs (not KDM6A/6B), when compared to H1693 Parental cells by qRT-PCR. Cyclophilin B was used as the endogenous control for qPCR normalization in both (D) and (E) panels.

Figure S6, Related to Figure 4

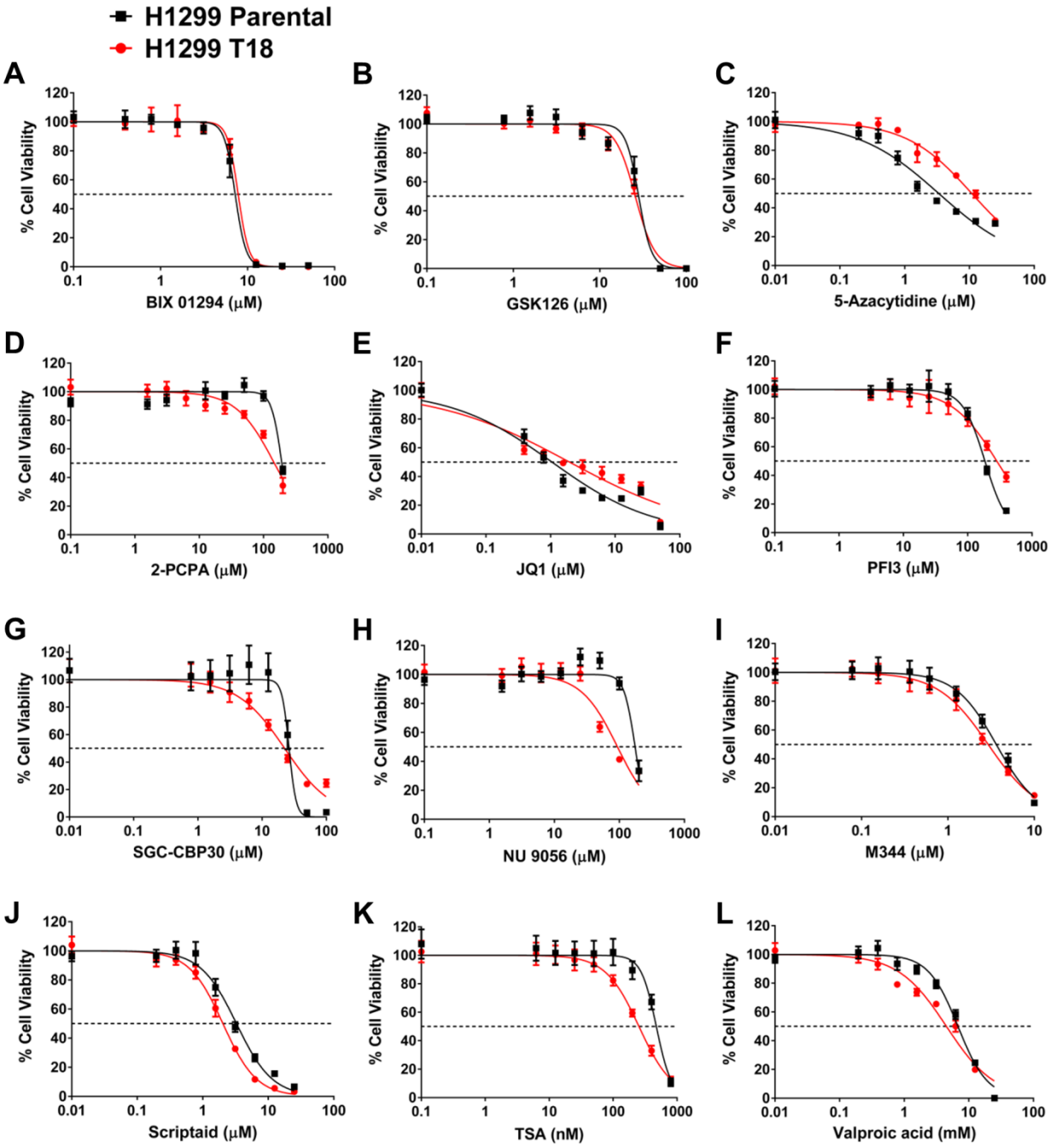

Figure S6. Response of H1299 T18 versus H1299 Parental to epigenetic inhibitors
H1299 T18 cells did not show hyper-sensitization to other classes of epigenetic drugs: Inhibitors of HMTs (A–C), LSD1 (D), BRD (E-G), HATs (H) or HDACs (I–L).

Figure S7, Related to Figure 5

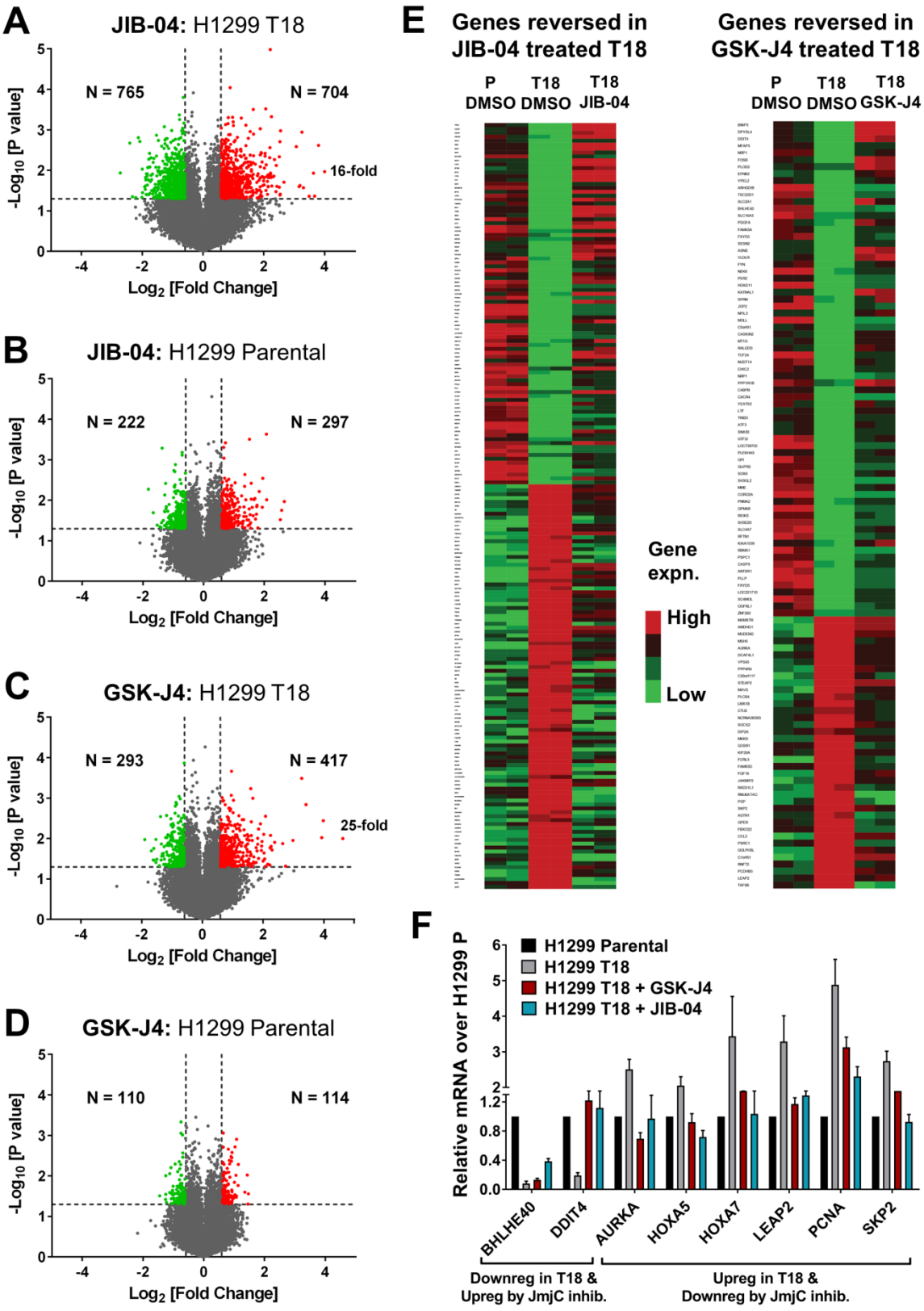

Figure S7. JIB-04 or GSK-J4 treated H1299 T18 cells selectively exhibit several transcriptional changes that are not seen in drug-treated H1299 Parental cells, and many of these alterations represent "reversal" of expression changes that were previously acquired upon development of taxane-platin resistance.

(A, B) H1299 T18 cells showed ~3-times greater gene expression changes (total 1469 probes) after 24 h treatment with 0.2 μM JIB-04, compared to H1299 Parental cells (519 probes). Top up-regulated gene in H1299 T18 showed ~16-fold expression difference.

(C, D) H1299 T18 cells showed ~3-times more drug-induced gene expression changes (total 710 probes) after 24 h treatment with 1 μM GSK-J4, compared to H1299 Parental cells (224 probes). Top up-regulated gene in H1299 T18 showed ~25-fold expression difference.

For (A-D) Red dots depict up-regulated genes and green dots represent down-regulated genes. All fold changes ≥ 1.5, t-test P values ≤ 0.05.

(E) Heat maps illustrate subset of genes altered by JIB-04 or GSK-J4 treatment that also represent "reversal" of expression changes that were acquired upon development of taxane-platin resistance in H1299 T18 vs H1299 Parental cells. Vertical lanes depict a total of 6 samples per heat map (2 biological replicates per treatment condition). About 195 Illumina probes (187 genes) were reversed in expression by 0.2 μM JIB-04 treatment and 110 Illumina probes (108 genes) showed reversed expression after 1 μM GSK-J4 treatment of H1299 T18 cells. Fold changes ≥ 1.5, t-test P values ≤ 0.05. Top reversed up-regulated (YPEL2) and top reversed down-regulated (LEAP2) genes by JIB-04 showed ~16-fold (up) and ~5-fold (down) changes respectively. Top reversed up-regulated (BNIP3) and top reversed down-regulated (TAF9B) genes by GSK-J4 showed ~10-fold (up) and ~3-fold (down) changes respectively. See Table S7 for complete lists of reversed genes.

(F) Select genes from microarray analysis in (E), whose expression was reversed by both JIB-04 and GSK-J4 were validated by qRT-PCR. 18S rRNA was used as the endogenous control for normalization.

Figure S8, Related to Figure 5

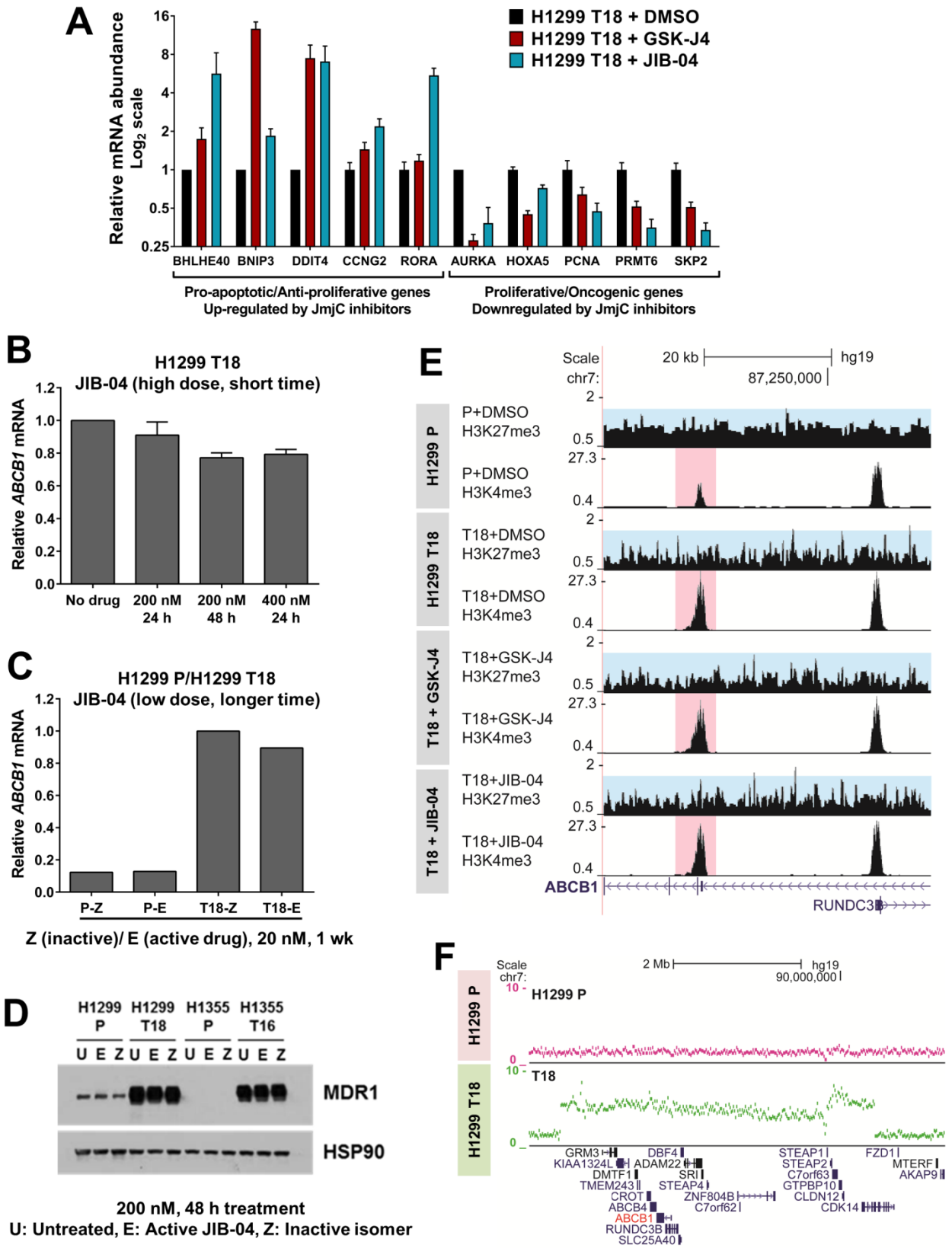

Figure S8. JmjC inhibitor treatment causes up-regulation of pro-apoptotic genes and down-regulation of proliferative genes, without altering MDR1 expression or histone methylation in short-term treated H1299 T18 cells.

(A) qRT-PCR revealed that several pro-apoptotic/ anti-proliferative genes were up-regulated and proliferative/ oncogenic genes were downregulated upon short-term 24 h treatment of H1299 T18 cells with JIB-04 (0.2 μM) or GSK-J4 (1 μM). 18S rRNA was used as the endogenous control for normalization.

(B) *ABCB1*/*MDR1* mRNA expression showed minimal change (only ~10-20% decrease) in H1299 T18 cells treated with high dose JIB-04 (10x-20x IC_{50} as determined by 96 h MTS assays) over a short period of time (24-48 h treatment).

(C) *ABCB1*/*MDR1* mRNA expression did not change much (only ~10-20% decrease) in H1299 T18 cells treated with low dose JIB-04 (1x IC_{50} as determined by 96 h MTS assays) over a longer period of time (1 wk treatment).

P: H1299 Parental cells, T18: H1299 T18 cells, E: Active JIB-04 isomer, Z: Inactive isomer.

(D) MDR1 protein levels in JmjC inhibitor-treated (200 nM JIB-04, 48 h) H1299 T18 and H1355 T16 cells remained at much higher levels than the parental cell lines.

(E) H3K4me3 (pink) and H3K27me3 (blue) enrichment at the *MDR1* locus in H1299 Parental, H1299 T18, GSK-J4 treated T18 and JIB-04 treated T18 cells. Although there was a decrease in H3K27me3 and increase in H3K4me3 at *ABCB1* locus in H1299 T18 vs H1299 Parental cells, these histone marks did not change after 24 h JmjC inhibitor treatment of H1299 T18 cells.

(F) *ABCB1*/*MDR1* locus was found to be genetically amplified in long-term paclitaxel + carboplatin treated H1299 T18 cells. Analysis was done using H1299 Parental and H1299 T18 input DNA samples from ChIP-seq dataset.

Figure S9, Related to Figure 6

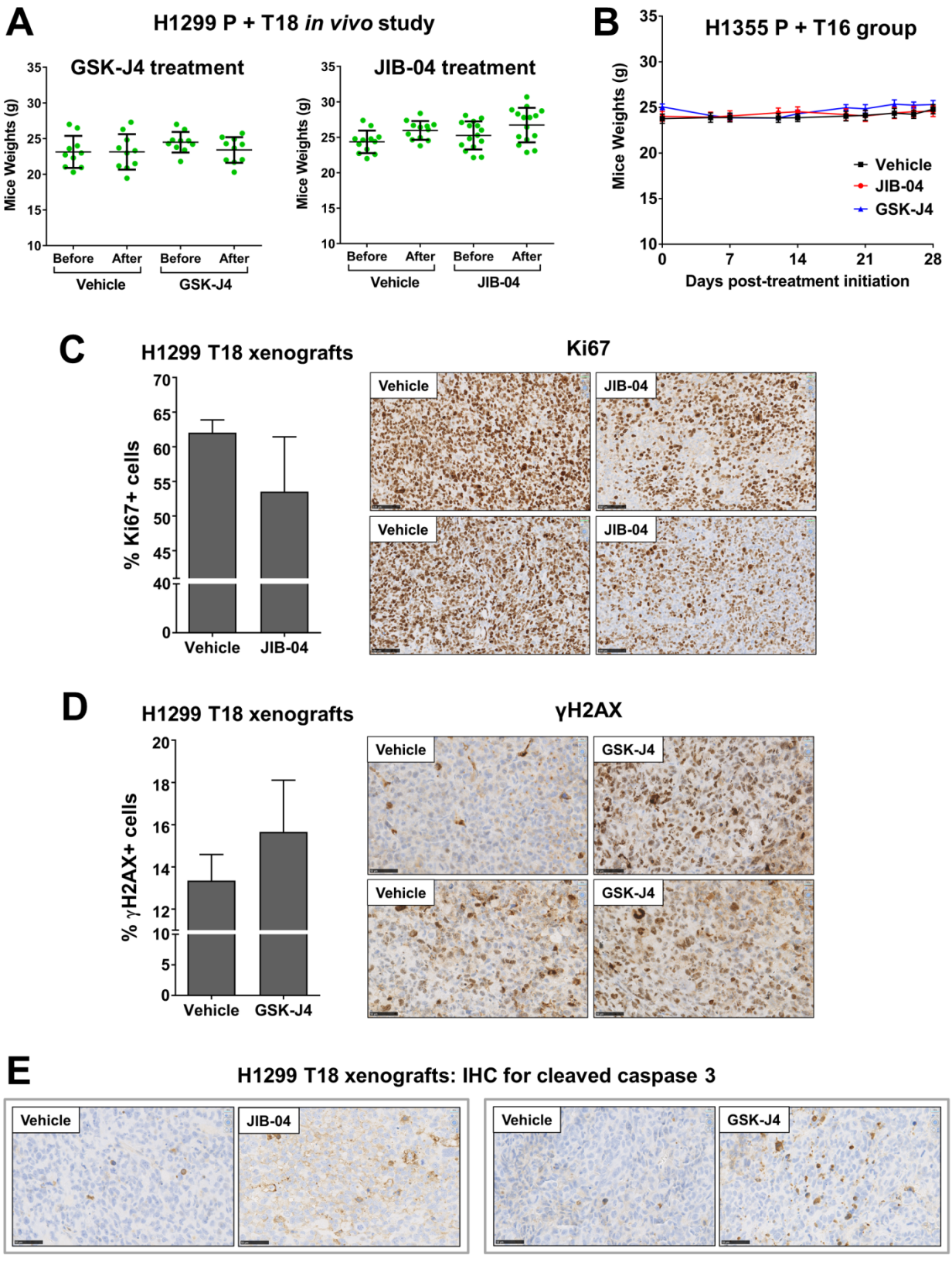

Figure S9. JmjC inhibitor treatment reduced cell proliferation and increased DNA damage in H1299 T18 xenografts, without causing any drug associated toxicity in mice receiving therapy.
(A) Body weights of mice bearing H1299 Parental or H1299 T18 xenograft tumors before and after JmjC inhibitor therapy. GSK-J4: 100 mg/kg i.p., for 10 consecutive days. JIB-04: 50 mg/kg, oral gavage, 3x per week, for 2 weeks.
(B) Body weights of mice bearing H1355 Parental or H1355 T16 xenograft tumors measured over the entire course of long-term JmjC inhibitor treatment. GSK-J4: 100 mg/kg i.p., 5x per week, for 4 weeks. JIB-04: 50 mg/kg, oral gavage, 3x per week, for 4 weeks.
(C) JIB-04 treatment caused reduction in % Ki67+ cells in H1299 T18 tumors *in vivo*, suggesting reduction in cell proliferation. Representative IHC images are shown. Scale bar: 100 μm
(D) GSK-J4 treatment increased % γH2AX+ cells in H1299 T18 tumors *in vivo*, indicating increased DNA damage. Representative IHC images are shown. Scale bar: 50 μm
For both (C-D): Percent positivity in the entire stained section per tumor was quantified via Aperio Image toolbox software. Data represents mean ± SEM of 3 tumors per group.
(E) JIB-04 and GSK-J4 treated H1299 T18 tumors exhibited focally increased cleaved caspase 3 staining (apoptotic marker) in some tumor regions. Representative IHC images are shown.

Supplemental Tables

Table S1. Clinical annotations and driver oncogenotypes of NSCLC cell lines; Related to Fig 1 and S3.

Clinical annotations:

Cell Line	NSCLC Subtype	Stage	Age	Race	Gender	Smoking Pack Years (PY)
NCI-H1299	Large Cell Carcinoma	IIIA	43	Caucasian	M	50
NCI-H1355	Adenocarcinoma	IV	53	Caucasian	M	100
NCI-H1693	Adenocarcinoma	IIIB	55	Caucasian	F	80
HCC4017	Large Cell Carcinoma	IA	62	Caucasian	F	Ex-smoker (76 PY)

Driver oncogenotypes:

Cell Line	TP53	KRAS	NRAS	LKB1	EGFR
NCI-H1299	HD	WT	Mutant	WT	WT
NCI-H1355	Mutant	Mutant	WT	Mutant	WT
NCI-H1693	Mutant	WT	WT	WT	WT
HCC4017	Mutant	Mutant	WT	WT	WT

WT, Wild-type
HD, Homozygous deletion

Table S2. Clinical annotations of NSCLC patient tumor dataset; Related to Fig 2.

	Chemo-treated [a] (before surgical resection; neoadjuvant)	**Chemo-naïve** (at the time of surgical resection)
Total	66	209
Platin + Taxane doublet [b]	56	-
Other platin-based doublets [c]	10	-
Diagnosis		
Adenocarcinoma	31	152
Squamous cell carcinoma	23	57
Other	12	0
Gender		
Males	36	112
Females	30	97
Stage		
I	18	115
II	15	35
III	28	58
IV	5	1
Smoking history		
Yes	58	186
No	8	20
Unknown	0	3
Race		
Caucasian	59	185
African American/ Asian/ Hispanic	7	24

[a] Neoadjuvant treated patient dataset was used for evaluating 35-gene pre-clinical resistance signature. Cancer-free survival data was available for 65 out of 66 patients. Hence one sample was excluded from clustering and cancer-free survival analyses shown in Figure 4. Annotation of excluded sample: Adenocarcinoma, Male, Stage IV, Non-smoking, and Caucasian.

[b] Carboplatin + Paclitaxel (N = 25), Cisplatin + Docetaxel (N = 24), Carboplatin + Docetaxel (N = 7)

[c] Carboplatin or Cisplatin with Etoposide/ Gemcitabine/ Pemetrexed/ Navelbine

Table S3. Cox multivariate regression on cancer-free survival analysis to test for bias from clinical covariates; Related to Fig 2.

	coef	exp(coef)	se(coef)	z	P value
Two Groups/ Clusters [a]	1.63	5.10	0.49	3.35	0.0008
Histology (Squamous)	-0.23	0.80	0.50	-0.46	0.64
Histology (Non Sq)	0.37	1.45	0.47	0.78	0.43
Age	0.02	1.02	0.03	0.88	0.38
Smoking history (Y)	-0.93	0.40	0.67	-1.39	0.16
Gender (M)	-0.21	0.81	0.43	-0.49	0.62
Race (Asian or Pacific Islander)	-0.28	0.76	1.52	-0.18	0.85
Race (Caucasian)	-0.87	0.42	0.80	-1.09	0.28
Race (Hispanic)	-0.13	0.88	1.29	-0.10	0.92
Adjuvant therapy (Y)	-1.03	0.36	0.50	-2.07	0.04
Neoadjuvant (Pac + Carb)	0.53	1.69	0.52	1.01	0.31
Stage (II)	-0.24	0.79	0.59	-0.40	0.69
Stage (III)	1.00	2.73	0.50	2.02	0.04
Stage (IV)	0.95	2.59	0.67	1.43	0.15

[a] Clustering of patients into two groups was the most significant contributor to the cancer-free survival difference (***P = 0.0008).

Table S4. Multivariate analysis of 35 gene signature towards poor cancer recurrence-free survival of neoadjuvant treated NSCLC patients; Related to Fig 2.

Genes	coef	exp(coef)	se(coef)	z	P value
KDM3B [a]	2.33	10.28	1.04	2.24	0.025
ADAM22	1.81	6.10	1.22	1.48	0.14
IMMP2L	0.64	1.89	0.76	0.84	0.40
NTN1	0.42	1.52	0.48	0.87	0.38
FAM133A	0.19	1.20	0.24	0.76	0.44
STX11	-0.06	0.94	0.41	-0.15	0.88
HEY2	-0.11	0.89	0.23	-0.50	0.62
HIGD2A	-0.15	0.86	1.15	-0.13	0.89
RUNDC3B	-0.17	0.84	0.37	-0.47	0.64
PPARGC1B	-0.34	0.71	0.39	-0.86	0.39
TTC1	-0.75	0.47	0.88	-0.85	0.40
ZNF672	-1.72	0.18	1.03	-1.67	0.094
STX8	-2.12	0.12	0.86	-2.47	0.014
CLINT1	-2.99	0.05	1.37	-2.18	0.029
NNT [b]	3.02	20.41	0.89	3.40	0.001
NXF2B	2.71	14.96	1.65	1.64	0.10
TRAF3IP2	1.36	3.89	0.90	1.52	0.13
DTX3	0.88	2.41	0.32	2.73	0.006
REXO2	0.82	2.28	1.08	0.76	0.44
LBX2	0.69	2.00	0.35	2.00	0.046
FUT4	0.70	2.00	0.85	0.82	0.41
GALNT13	0.52	1.68	0.38	1.37	0.17
CRIP1	0.48	1.62	0.41	1.18	0.24
TNC	0.45	1.58	0.27	1.68	0.092
MAGEA1	0.39	1.47	0.22	1.78	0.075
ANGPT1	0.21	1.23	0.35	0.59	0.55
RIN3	0.18	1.19	0.41	0.43	0.67
GALC	0.10	1.11	0.65	0.16	0.88
PLEK2	-0.09	0.92	0.27	-0.32	0.75
ZMAT3	-0.24	0.78	0.89	-0.27	0.79
LOC400027	-0.32	0.73	0.51	-0.62	0.54
DYNC2H1	-0.72	0.48	0.45	-1.61	0.11
ANP32B	-0.80	0.45	0.76	-1.06	0.29
FAM133B	-1.68	0.19	1.32	-1.27	0.20
NXF2	-1.96	0.14	1.31	-1.50	0.13

[a] KDM3B was up-regulated in resistant cell lines and xenografts, and showed the most significant, positive correlation with poor cancer recurrence-free survival (exp coeff/ Hazard ratio = 10.28, P value = 0.025)

[b] Though NNT expression had a high positive correlation in this multivariate analysis, it was actually down-regulated in our pre-clinical resistant models and was hence not selected for subsequent studies.

Table S5. Multivariate analysis for *KDM3A* and *KDM4A* expression data showing that the Neoadjuvant vs Chemo-naïve comparison was not biased by clinical variables; Related to Fig 3.

KDM3A

	Estimate	Std.Error	t value	Pr(>|t|)	
(Intercept)	4.687	0.706	6.638	3.85E-10	****
Neoadj ChemoTreated (Y)	**0.761**	**0.185**	**4.120**	**5.84E-05**	****
Gender (M)	0.077	0.162	0.471	0.638	
Race (Asian)	-0.286	0.600	-0.476	0.635	
Race (Caucasian)	-0.196	0.302	-0.650	0.517	
Race (Hispanic)	-0.137	0.540	-0.253	0.801	
Age	0.015	0.008	1.805	0.073	
Histology (Squamous)	0.376	0.173	2.172	0.031	*
Tobacco history (Y)	-0.173	0.326	-0.532	0.595	
Stage II	0.293	0.223	1.313	0.191	
Stage III	0.124	0.199	0.626	0.532	
Stage IV	-0.750	0.532	-1.410	0.160	

KDM4A

	Estimate	Std.Error	t value	Pr(>|t|)	
(Intercept)	4.770	0.606	7.866	3.63E-13	****
Neoadj ChemoTreated (Y)	**0.362**	**0.159**	**2.284**	**0.024**	*
Gender (M)	-0.094	0.139	-0.671	0.503	
Race (Asian)	0.016	0.516	0.030	0.976	
Race (Caucasian)	0.103	0.260	0.395	0.693	
Race (Hispanic)	0.072	0.463	0.155	0.877	
Age	-0.009	0.007	-1.324	0.187	
Histology (Squamous)	0.120	0.149	0.806	0.422	
Tobacco history (Y)	-0.116	0.280	-0.416	0.678	
Stage II	-0.039	0.192	-0.204	0.839	
Stage III	0.049	0.171	0.286	0.775	
Stage IV	-0.017	0.457	-0.037	0.971	

Table S6. Selectivity Ratio (SR*) of chemo-resistant cells to various standard, targeted and epigenetic therapies shows selective hypersensitization to Jumonji inhibitors; Related to Fig 4.

	Drug Class	Drugs	H1299 T18 SR	H1355 T16 SR
MDR1 substrates	Taxanes	Paclitaxel+Carboplatin	0.02	0.01
		Paclitaxel	0.03	0.02
		Docetaxel	0.03	0.002
	Anthracycline	Doxorubicin	0.04	0.25
	Vinca alkaloid	Vinorelbine	0.03	0.002
	HDAC	Depsipeptide	0.05	0.03
Other standard and targeted chemotherapies	NAMPT	FK866	0.1	2.1
	Platinum drug	Carboplatin	0.8	1.2
	Nucleoside metabolic + platin	Gemcitabine+Cisplatin	2.3	2.3
	Akt	MK-2206	0.7	1.8
	SMAC mimetic	JP1201	1.0	2.0
	Estrogen receptor agonist/antagonist	Tamoxifen	1.0	1.0
	Wnt	XAV939	2.7	1.0
	Topoisomerase	Irinotecan	1.1	2.7
	Bmi1/Ring1A	PRT 4165	1.0	1.4
Epigenetic drugs	2-OG oxygenases	IOX1	1.2	0.9
	DNMT	5-azacytidine	0.2	2.6
	Bromodomain	SGC-CBP30	1.3	0.9
		JQ1	0.6	6.6
		PFI 3	1.1	2.5
	HAT	NU 9056	2.0	1.0
	HDAC	M 344	1.1	1.8
		Valproic acid	1.4	1.3
		Scriptaid	1.5	1.4
		Trichostatin A	1.8	2.6
	HMT	BIX 01294	0.9	1.9
		DZNep	1.1	1.7
		GSK 126	1.0	0.8
	LSD1	2-PCPA	1.3	1.8
	JIB 04 Control	Z isomer (Inactive)	1.1	1.0
	JmjC KDMs	JIB-04 (E; Active)	20.3	2.8
		GSK J4	22.3	10.4

***Selectivity Ratio SR = [IC_{50} of Parental] / [IC_{50} of Resistant]**

SR < 1 implies that variant cell lines (H1299 T18 and H1355 T16) are cross-resistant to these drugs
SR = 1 indicates no change in drug response between parental and variant cell lines
SR > 1 implies sensitization of chemo-resistant variants to these drugs; values denote fold reduction in IC_{50} values

Table S7. Gene expression changes in H1299 T18 taxane-platin resistant vs H1299 Parental cells that were reversed by 24 h short-term JIB-04 (0.2 μM) or GSK-J4 (1 μM) treatment of H1299 T18 cells; Related to Figures 5 and S7.

Drug-treated samples were compared to DMSO-treated controls. t-test P values ≤ 0.05, Fold changes ≥ 1.5. Fold changes of top up-regulated and top down-regulated genes "reversed" in expression by JIB-04 or GSK-J4 treatment are shown at the top of the respective gene lists.

Downreg in T18 vs P + Upreg by JIB-04	**Downreg in T18 vs P + Upreg by GSK-J4**	**Upreg in T18 vs P + Downreg by JIB-04**	**Upreg in T18 vs P + Downreg by GSK-J4**
(87 genes)	**(69 genes)**	**(100 genes)**	**(39 genes)**
YPEL2 (16-fold upreg)	BNIP3 (~10-fold upreg)	LEAP2 (~5-fold down)	TAF9B (~3-fold down)
C5orf41	DPYSL4	SKP2	LEAP2
FBXO32	DDIT4	LOC100128191	PCDHB5
DDIT4	MFAP5	TRIM55	RNFT2
PER2	NRP1	RAB36	C1orf61
EGFR	FOSB	PCDHB5	GOLPH3L
NRP1	PLOD2	VASH2	PSRC1
BHLHE40	EFNB2	GPER	CCL2
DDIT3	YPEL2	FAM127C	FBXO22
CTGF	ARHGDIB	SFXN5	GPER
EFNB2	TSC22D1	KIAA0895	AGTR1
NFIL3	SLC2A1	ERI2	PGP
JUN	BHLHE40	CROT	SKP2
GRAMD1B	SLC16A3	FGF16	RNU6ATAC
MT1G	PDGFA	C10orf140	RAD51L1
LYPD1	FAM43A	JAKMIP2	JAKMIP2
PPP1R15A	FXYD5	RIMKLA	FGF16
TMEM91	ASNS	D2HGDH	FCRL3
BNC1	SESN2	NLRP11	FAM83D
TRIB3	VLDLR	ZKSCAN5	KIF20A
BMP2	NEK6	ISL1	GOSR1
RBMS1	FYN	HOXB5	MKKS
ATF3	PER2	MUDENG	DIP2A
RAB3IL1	HOXD11	NCRNA00085	SOCS2
CCDC93	KATNAL1	STEAP2	NCRNA00085
KRT86	SPRN	FAM83D	CTU2
WDR33	JDP2	GSTM4	LMX1B
ZNF442	NFIL3	LOC100132707	MAVS
SNX30	MGLL	LOC283683	PLCB4
ASNS	C5orf41	SERTAD4	STEAP2
RALGDS	CASKIN2	FBXL5	PPP4R4
SPRN	MT1G	DDX46	C20orf117
RAB4B	RALGDS	C1RL	AURKA
SAT1	TCF24	C6orf168	DCAF4L1
DCBLD2	NUDT14	WDR36	VPS45
CHIC2	CHIC2	KIF20A	MSH5
ZMYM5	PPP1R1B	PSRC1	MAMSTR
BEND7	C4BPB	C15orf52	AMDHD1
SH3GL2	CXCR4	RRM2	MUDENG
CCDC28A	YEATS2	LYRM7	
PTP4A3	LTF	BRI3BP	
TCP11L1	TRIB3	NFATC2IP	
PLAUR	ATF3	STRADB	
PVRL2	SNX30	C1R	
PLAU	GTF2I	LRRC8B	

WIPI1	LOC730755	FNTB	
SH3BP1	PLEKHA9	ATP2A2	
TCF24	GLIPR2	ZNF839	
LOC730755	GPI	C20orf117	
TMEM114	SOX8	LOC100127910	
AMOTL2	SH3GL2	GAS8	
TRAF4	MME	PRKX	
YEATS2	CORO2A	SATB2	
ATXN3	PNMA2	GK	
C9orf21	GPM6B	RNFT2	
HINFP	RIOK3	FLJ39061	
UBXN7	SH3D20	ATP8B2	
SCGB1A1	SLC4A7	MLKL	
RELB	RFTN1	SLC25A44	
RFTN1	RBMS1	BACH2	
ANTXR1	KIAA1539	HAS3	
PTHLH	PSPC1	SLC10A7	
PLLP	CASP9	ZNF618	
ATPBD4	ANTXR1	AP1G1	
CLCN6	PLLP	RPL23AP82	
VLDLR	LOC221710	TBX18	
CHEK2	SC4MOL	TOMM40L	
ZNF567	OGFRL1	RAD17	
NUDT14	ZNF260	C1orf61	
BAMBI		TXLNG	
ZNF529		TRAK2	
MED30		C18orf55	
JDP2		ABCB6	
ZNF259		PHF10	
BOD1		FARSB	
FGGY		NEFH	
CNOT4		SUPT16H	
MAGED2		REEP5	
NXN		SOCS4	
ZNF197		FAN1	
AKR1A1		HOXA10	
SLAIN1		PARD6G	
HPS1		GNA15	
GPM6B		ABCD3	
DENND1A		ATG2A	
KLK13		MARCKSL1	
PSPC1		FAM36A	
		PCYOX1	
		TSPAN12	
		CXXC4	
		L3MBTL2	
		PHTF1	
		AURKA	
		ARHGAP11A	
		RNF114	
		VPS45	
		ZC4H2	
		L3MBTL1	
		TMEM67	
		LACTB	

Table S8. 38 gene sets overlapping between the three GSEA analyses, representing depletion in H1299 T18 and enrichment/reversal by both JIB-04 and GSK-J4 treatments; Related to Fig 5.

Gene sets	Depleted in H1299 T18 vs P			Enriched by JIB-04 in T18			Enriched by GSK-J4 in T18		
	NES	p	FDR	NES	p	FDR	NES	p	FDR
Elvidge_Hypoxia_Up	-1.90	0.001	0.053	+2.52	0.000	0.000	+3.69	0.000	0.000
Elvidge_Hypoxia_By_DMOG_Up	-1.89	0.006	0.053	+2.75	0.000	0.000	+3.60	0.000	0.000
Martoriati_MDM4_Targets_Fetal_Liver_Up	-1.54	0.029	0.226	+2.65	0.000	0.000	+3.23	0.000	0.000
Jiang_Hypoxia_Normal	-1.51	0.029	0.241	+1.94	0.000	0.016	+3.03	0.000	0.000
Manalo_Hypoxia_Up	-1.97	0.000	0.039	+2.44	0.000	0.000	+2.83	0.000	0.000
Martoriati_MDM4_Targets_Neuroepithelium_Up	-1.83	0.001	0.064	+2.07	0.000	0.006	+2.61	0.000	0.000
Boquest_Stem_Cell_Cultured_Vs_Fresh_Up	-1.82	0.001	0.068	+2.87	0.000	0.000	+2.29	0.000	0.001
Monnier_Postradiation_Tumor_Escape_Dn	-1.66	0.013	0.134	+2.19	0.000	0.002	+2.24	0.000	0.001
Sweet_Lung_Cancer_KRAS_Dn	-1.52	0.033	0.231	+2.42	0.000	0.000	+2.18	0.000	0.003
Rozanov_MMP14_Targets_Up	-1.74	0.006	0.094	+1.41	0.107	0.185	+2.08	0.001	0.007
Dazard_Response_To_UV_NHEK_Up	-2.09	0.000	0.017	+2.50	0.000	0.000	+2.03	0.003	0.011
Acevedo_Liver_Cancer_Dn	-1.59	0.017	0.181	+1.32	0.140	0.249	+2.02	0.004	0.011
Gozgit_ESR1_Targets_Dn	-1.59	0.013	0.182	+2.39	0.000	0.000	+2.02	0.001	0.011
Acevedo_Liver_Tumor_Vs_Normal_Adjacent_Tissue_Dn	-1.50	0.057	0.240	+2.14	0.000	0.004	+2.01	0.001	0.011
Pedersen_Metastasis_By_ERBB2_Isoform_7	-1.54	0.024	0.224	+1.50	0.069	0.132	+2.01	0.004	0.012
Martens_Bound_By_PML_RARA_Fusion	-1.67	0.008	0.135	+1.73	0.025	0.048	+1.93	0.007	0.019
Schaeffer_Prostate_Development_48hr_Dn	-1.54	0.038	0.219	+1.35	0.134	0.224	+1.90	0.007	0.024
Wong_Adult_Tissue_Stem_Module	-1.97	0.000	0.038	+1.97	0.001	0.012	+1.82	0.012	0.038
Koyama_SEMA3B_Targets_Up	-3.21	0.000	0.000	+1.51	0.066	0.128	+1.81	0.011	0.041
Lim_Mammary_Stem_Cell_Up	-1.78	0.000	0.077	+2.13	0.000	0.004	+1.74	0.031	0.059
Sweet_Lung_Cancer_KRAS_Up	-1.73	0.004	0.096	+1.57	0.042	0.099	+1.72	0.026	0.063
Onder_CDH1_Targets_2_Dn	-1.98	0.000	0.036	+2.40	0.000	0.000	+1.72	0.030	0.063
Fulcher_Inflammatory_Response_Lectin_Vs_Lps_Up	-1.74	0.001	0.097	+2.47	0.000	0.000	+1.71	0.020	0.065
Plasari_TGFB1_Targets_10hr_Up	-1.63	0.032	0.161	+2.33	0.000	0.001	+1.71	0.017	0.066
Perez_TP63_Targets	-1.55	0.033	0.214	+1.74	0.019	0.047	+1.69	0.032	0.073
Bruins_UVC_Response_Via_TP53_Group_B	-1.92	0.000	0.050	+1.45	0.080	0.161	+1.67	0.028	0.080
Enk_UV_Response_Keratinocyte_Up	-1.84	0.000	0.064	+2.65	0.000	0.000	+1.63	0.030	0.091
Schuetz_Breast_Cancer_Ductal_Invasive_Up	-1.90	0.000	0.053	+2.54	0.000	0.000	+1.63	0.043	0.092
West_Adrenocortical_Tumor_Dn	-1.56	0.012	0.205	+1.91	0.008	0.018	+1.62	0.034	0.095
Delys_Thyroid_Cancer_Up	-1.91	0.002	0.051	+1.85	0.009	0.024	+1.54	0.056	0.129
Martens_Tretinoin_Response_Up	-1.95	0.000	0.045	+1.41	0.088	0.187	+1.52	0.060	0.136
Chicas_RB1_Targets_Senescent	-1.84	0.002	0.065	+1.73	0.023	0.048	+1.51	0.077	0.139
Lei_MYB_Targets	-1.92	0.000	0.052	+1.44	0.106	0.167	+1.49	0.072	0.154
Meissner_Brain_HCP_With_H3K4me3_And_H3K27me3	-1.68	0.000	0.122	+1.93	0.003	0.016	+1.43	0.090	0.186
Naba_Matrisome	-2.20	0.000	0.006	+2.05	0.002	0.007	+1.43	0.103	0.186
Benporath_SUZ12_Targets	-1.89	0.000	0.054	+1.99	0.003	0.011	+1.41	0.115	0.196
Lindgren_Bladder_Cancer_Cluster_2b	-1.87	0.000	0.058	+1.42	0.092	0.179	+1.40	0.126	0.196
Pasini_SUZ12_Targets_Dn	-1.53	0.021	0.227	+2.16	0.002	0.003	+1.34	0.147	0.244

Gene Set Enrichment Analysis (GSEA) was performed using the GSEAPreranked tool to analyze ranked lists of differentially expressed genes from microarray analyses (fold change ≥ 1.5, t-test P value ≤ 0.05) against curated gene sets (C2) from the Molecular Signatures Database v5.0/ MSigDB (Subramanian et al., 2005).

NES: Normalized Enrichment Scores, p = Nominal p value, FDR: False Discovery Rate
1000 gene set permutations, FDR ≤ 0.25

Supplemental Experimental Procedures

Drugs

Cell lines were tested for response to several drugs including paclitaxel (Bedford Labs/Hikma Pharmaceuticals and also from Hospira, Lake Forest, IL), carboplatin (Sandoz Inc., Princeton, NJ and from Sagent Pharmaceuticals, Schaumburg, IL), docetaxel (LC Laboratories, Woburn, MA), cisplatin (APP Pharmaceuticals, Schaumburg, IL), doxorubicin (Teva Parenteral, Irvine, CA), vinorelbine (Pierre Fabre Company, Castres, France), irinotecan hydrochloride (Sandoz Inc., Princeton, NJ), gemcitabine (Eli Lilly and Company, Indianapolis, IN), pemetrexed (Eli Lilly and Company, Indianapolis, IN), fludarabine (Selleck Chemicals, Houston, TX), verapamil (Sigma-Aldrich), PGP-4008 (Santa Cruz Biotechnology), depsipeptide/ romidepsin (ApexBio, Houston, TX), trichostatin A (Sigma-Aldrich, St. Louis, MO), GSK126 (Xcess Biosciences, San Diego, CA) and JIB-04 (Synthetic chemistry core at UT Southwestern). NU 9056, PFI 3, PRT 4165, SGC-CBP30, GSK-J5 and GSK-J4 were from Tocris Bioscience (Bristol, UK).

Colony formation assays

Cells were counted using a Beckman Coulter Z2 Particle Count and Size Analyzer, and plated at a density of 400 cells per well of a 6-well plate. Cells were treated the next day with serial dilutions of chemotherapeutic drug. Plates were kept in the cell culture incubator until termination of assay. After 2-3 weeks, colonies were stained with crystal violet staining solution (0.5% crystal violet, 3% formaldehyde solution), rinsed in water and imaged. Colonies were counted both manually and automatically using Quantity One image analysis software (Bio-Rad).

Testing emergence of drug-tolerant colonies from mass population

10,000-20,000 cells were plated per well of a 6-well plate. Cells were allowed to attach and drug treatment was given the next day. Sub-lethal doses used for each epigenetic compound were pre-determined in colony formation assays as indicated in the figures. Doses were restricted to $\leq$10 μM. Colonies were grown until no treatment wells were confluent (2 weeks for H1299, 3-5 weeks for other lines). At the end of the assay, wells were stained with crystal violet staining solution (0.5% crystal violet, 3% formaldehyde solution), rinsed in water and imaged using Quantity One (Bio-Rad).

In vivo studies

For Fig 1I-J, 6-8 week old female NOD/SCID mice (UTSW breeding core) were used. For all subsequent *in vivo* studies (Fig 6,7), 6 week old female athymic nude mice were used (Charles River or Jackson Lab). Cell lines were trypsinized, washed and counted using Beckman Coulter counter. Cell viability was assessed using trypan blue to ensure >95% viability prior to injections. For studies with H1299 Parental or T18 cell lines, injections were done with 1 million cells suspended in PBS or RPMI, and for H1355 Parental or T16 cells, 4-5 million cells in 1:1 RPMI: matrigel were injected subcutaneously into the right flank of mice. Tumor growth was monitored by caliper measurements and tumor volume was calculated as (0.5 x length x width^2). Drug/Vehicle therapy was given to tumor volume matched pairs. Treatment was started when tumors reached ~150-200 mm^3, unless otherwise stated.

Docetaxel +Cisplatin therapy: Mice received either both vehicle treatments or docetaxel (3 mg/kg, dissolved in DMSO-ethanol mix and diluted in saline) and cisplatin (3 mg/kg in saline) i.p. injections, once a week for 3 weeks.

JIB-04: Mice were randomized to receive either of 5, 20 or 50 mg/kg JIB-04 doses or vehicle (12.5% cremophor EL, 12.5% DMSO, aqueous suspension), given by oral gavage, 3x/week for 2 weeks. For Fig 6H, starting at 120 mm^3 tumor volume, mice received 50 mg/kg JIB-04, 3x/week for 4 weeks.

GSK-J4: For Fig 6A-B, mice were given vehicle or 100 mg/kg GSK-J4 (R&D Systems, dissolved in 100% DMSO), given i.p., every day for 10 consecutive days, as documented previously (Hashizume et al., 2014). For Fig 6H, starting at 120 mm^3 tumor volume, mice received 100 mg/kg GSK-J4, 5x/week for 4 weeks.

Paclitaxel + Carboplatin combined with JmjC inhibitors: For Fig 7E, treatment was started at ~100 mm^3. Paclitaxel (from Hospira Inc., IL, diluted in saline, 20 mg/kg) + Carboplatin (aq. solution from Pharmachemie B.V., The Netherlands, diluted in water, 30 mg/kg), were both given i.p. on the same day, 1x per week. Mice in vehicle control group also received two i.p. vehicle injections on the same day. Following a one day break, mice in combination treatment groups received either JIB-04 (5 mg/kg), by oral gavage or GSK-J4 (Selleckchem Cat# S7070, dissolved in 25% DMSO: aq. suspension, 100 mg/kg), by i.p. injection, 3x per week. JIB-04 vehicle or GSK-J4 vehicle were administered at the same time to control mice.

Immunohistochemistry (IHC) of xenograft tumors
Immunohistochemical analysis was performed on a Dako Autostainer Link 48 system. Briefly, the slides were baked for 20 minutes at 60°C, then deparaffinized and hydrated before the antigen retrieval step. Heat-induced antigen retrieval was performed in a Dako PT Link for 20 minutes at a pH of 6.1 for Ki67 staining and at a pH of 9 for cleaved caspase 3 and γH2AX. The tissue was incubated with a peroxidase block and then with the antibody against Ki67 (Dako, cat# 1R626, RTU), cleaved caspase 3 (Cell Signaling, cat# 9661, 1:1500 dilution) or γH2AX (Millipore, cat# 05-636, 1:1000 dilution) for 20 minutes. The staining was visualized using the EnVision FLEX visualization system. Slides were scanned using the NanoZoomer digital slide scanner (Hamamatsu) and visualized using the NDPview2 software. Slides were also scanned in an Aperio AT2 scanner for quantitative analysis using Aperio Image toolbox software (Leica Biosystems).

NSCLC patient tissue microarray (TMA)
FFPE tumor tissues were used to construct NSCLC tissue microarray #3 (TMA3) for immunohistochemistry. IHC staining was done using a Leica Bond autostainer, with rabbit monoclonal antibody for KDM3B (Cell Signaling Technology, clone C6D12, cat #3100, dilution 1:80). A human colon adenocarcinoma specimen was used as positive control. Stained samples were assigned an expression score by the pathologist.

Microarray data analysis
Log ratios, unpaired t-test p values and color-coded heat maps were obtained using MATRIX. For comparisons involving progressively resistant cell line series, analyses were performed using R package by fitting linear regression model on gene expression data against the log transformed IC50 values as measures of drug response. We fitted beta-uniform mixture model to a set of p-values using the R package ClassComparison. Genes with p-values below the FDR cutoff of 0.1 were considered statistically significant. For xenograft data, differential gene expression analysis was performed by student's t-test. Using 35 gene signature, unsupervised hierarchical clustering (Eisen et al., 1998) was performed to separate neoadjuvant chemotherapy treated patients into two groups. Clustering was based on Euclidean distance matrix and maximum linkage method. Kaplan-Meier survival analysis and multivariate Cox regression were performed by R survival package and replotted using Graphpad Prism 6.00 (GraphPad Software, La Jolla, California USA). R code is provided in Sweave report.

Gene Set Enrichment Analysis (GSEA)
Ranked lists of differentially expressed genes from microarray analyses (fold change ≥ 1.5, t-test P value ≤ 0.05) were assessed through the GSEA desktop application (http://www.broadinstitute.org/gsea/downloads.jsp) using the GSEAPreranked tool. Curated gene sets (C2) from the Molecular Signatures Database v5.0/ MSigDB (Subramanian et al., 2005) were interrogated. After filtering out genes that were not in the expression dataset, gene sets smaller than 15 genes or larger than 3000 genes were excluded from analysis. GSEA was run using 1000 gene set permutations to generate False Discovery Rate (FDR). Default settings were used for normalizing the enrichment scores (NES).

Histone PTM Mass Spectrometry Analysis
NSCLC cells were harvested and histones extracted from cell pellets as described (Sidoli et al., 2016) or using EpiQuik™ Total Histone Extraction kit (cat# OP-0006). A total of 3 biological replicates per cell line were used for mass spectrometry. Histones were prepared for mass spectrometry by chemical derivatization using propionic anhydride and digested to peptides with trypsin, followed by another round of derivatization. Peptides were desalted using C18 stage-tips and about 1-2ug peptides were analyzed using an EASY-nLC nanoHPLC (Thermo Scientific, Odense, Denmark) coupled with a Q-Exactive mass spectrometer (Thermo Fisher Scientific, Bremen, Germany). HPLC gradients and mass spectrometry parameters are defined previously (Bhanu et al., 2016). To facilitate MS/MS-based quantification, both data-dependent acquisition and targeted acquisition for isobaric peptides were included. The relative abundance of histone H3 and H4 peptides were calculated by using EpiProfile (Sidoli et al., 2016).

ChIP-Sequencing of Histone H3K4me3 and H3K27me3
H1299 parental and T18 cells at 80% confluency (~$1x10^7$) were cross-linked with 1% formaldehyde for 10 minutes at 37°C, and quenched with 125 mM glycine at room temperature for 5 minutes. The fixed cells were washed twice with cold PBS, scraped, and transferred into 5 ml PBS containing Mini EDTA-free protease inhibitors (Roche). After centrifugation at 700 g for 4 minutes at 4°C, the cell pellets were resuspended in 1.5 ml ChIP lysis buffer (1% SDS, 10 mM EDTA, 50 mM Tris-HCl [pH 8.1] with protease inhibitors) and sonicated at 4°C with a Bioruptor

(Diagenode) (30 seconds ON and 30 seconds OFF at highest power for 2 x 15 minutes). The chromatin predominantly sheared to a fragment length of ~250 – 750 bp was centrifuged at 20,000 g for 15 minutes at 4°C. 100 µl of the supernatant was used for ChIP, and DNA purified from 30 µl of sheared chromatin was used as input. A 1:10 dilution of the solubilized chromatin in ChIP dilution buffer (0.01% SDS, 1.1% Triton X-100, 1.2 mM EDTA, 167 mM NaCl 16.7 mM Tris-HCl [pH 8.1]) was incubated at 4°C overnight with 10 µg of a rabbit polyclonal anti-Histone H3K4me3 antibody (Millipore, cat# 07-473) or a mouse monoclonal anti-Histone H3K27me3 antibody (Abcam, cat# ab6002). Immunoprecipitation was carried out by incubating with 40 µl pre-cleared Protein G Sepharose beads (Amersham Bioscience) for 1 hour at 4°C, followed by five washes for 10 minutes with 1ml of the following buffers: Buffer I: 0.1% SDS, 1% Triton X-100, 2 mM EDTA, 20 mM Tris-HCl [pH 8.1], 150 mM NaCl, protease inhibitors; Buffer II: 0.1% SDS, 1% Triton X-100, 2 mM EDTA, 20 mM Tris-HCl [pH 8.1], 500 mM NaCl, protease inhibitors; Buffer III: 0.25 M LiCl, 1% NP-40, 1% deoxycholate, 1 mM EDTA, 10 mM Tris-HCl [pH 8.1]; twice with TE buffer [pH 8.0]. Elution from the beads was performed twice with 100 µl ChIP elution buffer (1% SDS, 0.1 M NaHCO3) at room temperature (RT) for 15 minutes. Protein-DNA complexes were de-crosslinked by heating at 65°C in 192 mM NaCl for 16 hours. DNA fragments from immunoprecipitated chromatin and input were purified using QiaQuick PCR Purification kit (QIAGEN) and eluted into 30 µl H_2O according to the manufacturer's protocol after treatment with RNase A and Proteinase K.

For ChIP-Seq, barcoded libraries of ChIP and input DNA were generated with the TruSeq® ChIP Sample Preparation Kit (Illumina), and 50-nt single-end reads were generated with the HiSeq2000 system (Illumina). Sequence reads were aligned to the human reference genome (hg19) using Bowtie2 (v.2.2.5) (Langmead et al., 2009). All figures shown are normalized to the number of mapped reads to ensure that sequencing depth does not influence analysis. Additionally, we used minimal PCR cycles to mitigate bias which yielded ChIP-seq data of high quality as corroborated by low frequency of duplicate reads. Uniquely mapped reads with ≤2 mismatches to the reference sequence were retained for further analysis; for H1299 parental H3K27me3 and H1299 T18 H3K27me3 we obtained 26,100,406 and 29,586,658 reads, respectively, for H1299 parental H3K4me3 and H1299 T18 H3K4me3 we obtained 23,042,015 and 22,883,901 reads, respectively and for H1299 parental input and H1299 T18 input we obtained 26,995,155 and 25,187,823 reads, respectively. ChIP-Seq enrichment plots were generated using ngs.plot tool (Shen et al., 2014). Aligned bam files are provided as input to Ngs.plot to calculate read count per million mapped reads over all the ENSEMBL annotated gene body regions in the human genome. For each ChIP-Seq sample, the average signal in -2kb with respect to transcription start site (TSS), gene body and 2kb downstream of transcription end site (TES) regions were subtracted from respective input sample signal and visualized in the enrichment plot. For calling "bivalent" genes, genes were classified as bivalent if both H3K4me3 and H3K27me3 enriched regions fell in the range 500bp upstream or downstream of the TSS. Presence of H3K4me3 or H3K27me3 mark was defined by ≥4-fold average signal over input in this TSS±500bp region. Bivalency was considered to be "lost" if either of H3K4me3 or H3K27me3 signals dropped to <4-fold over input. Genes were said to have "regained" bivalent status if the lost mark showed at least a 1.5-fold increase in drug-treated versus DMSO-treated cells. All ChIP-seq datasets have been deposited under GEO accession number **GSE81689**.

RNA-Sequencing

H1299 Parental and T18 cells at 80% confluency were pelleted, snap-frozen and stored at -80^{0}C. Total RNA was extracted using RNeasy Plus Mini kit (Qiagen, Valencia, CA), with a gDNA eliminator step. RNA quality check was performed using the Agilent 2100 Bioanalyzer to ensure that only high quality RNA was used (RIN Score 8 or higher). The Qubit fluorometer (Invitrogen) was used to determine RNA concentration prior to library preparation with the TruSeq Stranded Total RNA LT Sample Prep Kit (Illumina). Samples were run on the Illumina HiSeq 2500, at the McDermott Sequencing Core at UT Southwestern. For RNA-Seq analysis, TopHat was used for transcript assembly, and the Cufflinks suite was used for differential expression calling and calculation of Fragments Per Kilobase of transcript per Million mapped reads (FPKM). All RNA-seq datasets have been deposited under GEO accession number **GSE81689**.

Histone demethylase activity assays

For quantification of histone demethylase activity in tumor lysates, tumor homogenates in PBS were sonicated (3x 4 sec) and equal amounts of protein were incubated with either a histone H3K4me3 or H3K9me3 or H3K27me3 substrate in a reaction buffer containing cofactors for 2h at 37°C before specific immuno-detection of the H3K4me2 or H3K9me2 or H3K27me2 products respectively, using Epigentek kit P-3081 (K9) or P-3083 (K4) or P-3085 (K27) reagents.

Flow cytometry
Cells were incubated with FITC- or APC-conjugated antibodies or appropriate isotype control antibody (BD Biosciences) at 4°C for 30 min in dark. Cells were washed, resuspended in HBSS+ and stained with Propidium Iodide before flow cytometry. For cell cycle analysis, briefly cells were fixed in cold 70% EtOH and incubated at 37°C for 30 min in staining buffer containing 50 µg/ml Propidium Iodide, 50 µg/ml RNAse A, 0.05% Triton X-100 and PBS. Flow cytometric profiling was performed on a FACScan or FACSCalibur flow cytometer (BD Biosciences) and analyzed using FlowJo software (Treestar).

Tritiated docetaxel accumulation assay
Cells were exposed to [^{3}H]-docetaxel for different time-points. Protein lysates were collected and quantified using BCA reagent. Samples were scintillated with Ecolume™ liquid scintillation cocktail. Drug accumulation was calculated as CPM/ mg protein.

siRNA knockdown
ABCB1 knockdown was achieved using three individual *ABCB1* siRNAs (Qiagen) and Lipofectamine RNAiMax (Invitrogen), following standard reverse transfection protocols.

Quantitative RT-PCR
Total RNA was isolated using RNeasy Plus Mini kit (Qiagen) and cDNA was generated using iScript cDNA synthesis kit (BioRad). For epigenetic enzymes tabulated below, transcripts were detected by SYBR Green chemistry in real time quantitative PCR assays using validated primers. Cyclophilin B was used as the endogenous control. For non-epigenetic transcripts, TaqMan assays (Life Technologies) were used, with 18S as the endogenous control. A reference sample containing pooled RNA from normal human and tumor tissues (Stratagene) was also used. PCR reactions were run using the ABI 7300 Real-time PCR System and analyzed with the included software. The comparative C_T method was used to compute relative mRNA expression.

SYBR Green Primers for Histone Lysine Demethylase Genes:

	Forward/ Reverse Primer Sequence	**RefSeq#**
KDM1A	CTAATGCCACACCTCTCTCAACTC	NM_015013.2
	CTAATGCCACACCTCTCTCAACTC	NM_015013.2
KDM2A	TCCACCGGCTGATAAACCA	NM_012308.1
	AGCCGGAAGTCGGTCATGT	NM_012308.1
KDM2B	GCGCTCCCACCTCACTCA	NM_001005366.1
	CCGAAGAGAAGCCGTCTATGC	NM_001005366.1
KDM3A	GTGGTTTTCAGCAACCGTTATAAA	NM_018433.4
	CAGTGACGGATCAACAATTTTCA	NM_018433.4
KDM3B	TGCCCTTGTATCAGTCGACAGA	NM_016604.3
	GCACTAGGGTTTATGCTAGGAAGCT	NM_016604.3
KDM3C	TCTTCACCCGCACCATGAT	NM_004241.2
	AGACCTGCGTCGTGATGTAATG	NM_004241.2
KDM4A	TGCAGATGTGAATGGTACCCTCTA	NM_014663.2
	CACCAAGTCCAGGATTGTTCTCA	NM_014663.2
KDM4B	GGCCTCTTCACGCAGTACAATAT	NM_015015.2
	CCAGTATTTGCGTTCAAGGTCAT	NM_015015.2
KDM4C	GAATGCTGTCTCTGCAATTTGAGA	NM_015061.2
	CAACGGCGCACATGACAT	NM_015061.2
KDM4D	CTGGGTGTATCCTCTGCATATAGAAC	NM_018039.2

	GCAGAGAATGTCCTCAGTGTTTAGAA	NM_018039.2
KDM5A	TGTGTTGAGCCAGCGTATGG	NM_005056.2
	CCACCCGGTTAAAAGCAGACT	NM_005056.2
KDM5B	TCCATCAGCTTGTGACCATCAT	NM_006618.3
	GTGGTAGGCTCTTGGAAATGTAATC	NM_006618.3
KDM5C	GAGGAGGGCTCAGGTAAGAGAGA	NM_004187.3
	TGGCAACAGCGAGGACAG	NM_004187.3
KDM5D	CAACCATGCAACTTCGAAAGAA	NM_001653.3
	CCCCACGGGAGCATACTTG	NM_001653.3
KDM6A	CACAGTACCAGGCCTCCTCATT	NM_021140.2
	TCACTATCTGAGTGGTCTTTATGATGACT	NM_021140.2
KDM6B	CGGAGACACGGGTGATGATT	NM_001080424.1
	CAGTCCTTTCACAGCCAATTCC	NM_001080424.1
KDM7A	GTCCATGGGAAGAGGACATCTT	NM_030647.1
	GATCATTATCTTTCGCTCTCCATTC	NM_030647.1
JARID2	TGTTCACAACGGGCATGTTT	NM_004973.2
	TTGTGTTTTTGAACAGGTTCCTTCT	NM_004973.2

Supplemental References

Bhanu, N. V., Sidoli, S., and Garcia, B. A. (2016). Histone modification profiling reveals differential signatures associated with human embryonic stem cell self-renewal and differentiation. Proteomics *16*, 448-458.

Eisen, M. B., Spellman, P. T., Brown, P. O., and Botstein, D. (1998). Cluster analysis and display of genome-wide expression patterns. Proceedings of the National Academy of Sciences of the United States of America 95, 14863-14868

Hashizume, R., Andor, N., Ihara, Y., Lerner, R., Gan, H., Chen, X., Fang, D., Huang, X., Tom, M. W., Ngo, V.*, et al.* (2014). Pharmacologic inhibition of histone demethylation as a therapy for pediatric brainstem glioma. Nat Med *20*, 1394-1396.

Langmead, B., Trapnell, C., Pop, M., and Salzberg, S. L. (2009). Ultrafast and memory-efficient alignment of short DNA sequences to the human genome. Genome biology *10*, R25.

Shen, L., Shao, N., Liu, X., and Nestler, E. (2014). ngs.plot: Quick mining and visualization of next-generation sequencing data by integrating genomic databases. BMC genomics *15*, 284.

Sidoli, S., Bhanu, N. V., Karch, K. R., Wang, X., and Garcia, B. A. (2016). Complete Workflow for Analysis of Histone Post-translational Modifications Using Bottom-up Mass Spectrometry: From Histone Extraction to Data Analysis. Journal of visualized experiments : JoVE.

Subramanian, A., Tamayo, P., Mootha, V. K., Mukherjee, S., Ebert, B. L., Gillette, M. A., Paulovich, A., Pomeroy, S. L., Golub, T. R., Lander, E. S., and Mesirov, J. P. (2005). Gene set enrichment analysis: a knowledge-based approach for interpreting genome-wide expression profiles. Proceedings of the National Academy of Sciences of the United States of America *102*, 15545-15550.